Journal of Information Display, Vol. 10, No. 4, December 2009 (ISSN 1598-0316)

Reduction of Temporal Image Sticking in AC Plasma Display Panels through the Use of High He Contents

Choon-Sang Park**, **Sun Ho Kim****, **Jae-Hyun Kim****, **and Heung-Sik Tae***

Abstract

The temporal dark- and bright-image sticking phenomena were examined relative to the He contents under 11% Xe content in the 50-in HD and FHD AC-PDPs with a ternary gas mixture (Xe-He-Ne). To compare the temporal dark- and bright-image sticking phenomena under various He contents, the differences in the disappearing time, display luminance, perceived luminance, infrared emission, color coordinate, color temperature, and discharge current before and after discharge were measured under 0, 35, 50, and 70% He contents. It was found that temporal dark- and bright-image sticking were reduced in proportion to the increase in He %. Thus, a high He content contributes to the reduction of temporal dark- and bright-image sticking.

Keywords: temporal dark- and bright-image sticking, AC-PDP, high He contents, IR emission, luminance, perceived luminance, discharge current, color temperature

1. Introduction

Since the invention of AC-PDPs in the 1960s by Coordinated Science Laboratory at the University of Illinois, extensive research has produced high-quality PDPs, enabling the current PDPs to claim a large market share in the flat-panel-display area [1-6]. The issue of image sticking or image retention recently emerged, however, which needs an urgent solution for the realization of a high image quality in IPTV (Internet protocol television), PID (public-information display), and electronic copyboards. Nonetheless, the image-sticking or image retention problems of PDPs remain in other display devices (e.g., cathode ray tubes [CRTs]; liquid crystal displays [LCDs]; and organic light-emitting diodes [OLEDs]). Image retention pertains to temporal image sticking that is easily recoverable through a minor treatment whereas image sticking is permanent and is not recoverable in spite of severe treatment. The sputtering phenomenon on the MgO surface caused by the ion bombardment during a repetitive strong sustain discharge causes severe aggravation on both the MgO surface and the phosphor layer, eventually resulting in a permanent image-sticking problem [7-11].

In the previous related research, the high He contents in the ternary gas composition (Ne-Xe-He) contributed to lower power consumption and high luminous efficiency [2]. No researches have yet been conducted, however, on the He gas contents for image sticking. Several efforts to reduce temporal image sticking have been reported, such as driving waveforms, the face-to-face structure, and the vacuum-sealing method [3-6]. Accordingly, this work investigates the temporal dark- and bright-image sticking problems, also known as image retention, under various He contents in 50-in HD and FHD AC-PDPs. As commercial 50-in AC-PDP modules use 11% Xe gas contents, the Xe content in this study was fixed at 11%.

2. Experimental Set-up

Fig. 1 shows the schematic diagram of the experimental setup that was used in this study. The commercial 50-in HD and FHD AC-PDP modules with three electrodes (X, Y, and A) were used to monitor the temporal dark- and bright-image sticking, where the square-type pattern was displayed. The square-type image was displayed on the screen using a pattern generator. The luminance, color coordinate, and color temperature were measured using a color

Manuscript Received December 02, 2009; Revised December 14, 2009; Accepted for publication December 24, 2009
This work was supported in part by the IT R&D program of MKE/KEIT and in part by Brain Korea 21 (BK21).
* Member, KIDS; ** Sutdent Member, KIDS
Corresponding author: Heung-Sik Tae
School of Electrical Engineering and Computer Science, Kyungpook National University, 1370 Sankyuk-Dong, Buk-Gu, Deagu 702-701, Republic of Korea
E-mail: hstae@ee.knu.ac.kr **Tel**: +82-53-950-6563 **Fax**: +82-53-950-5505

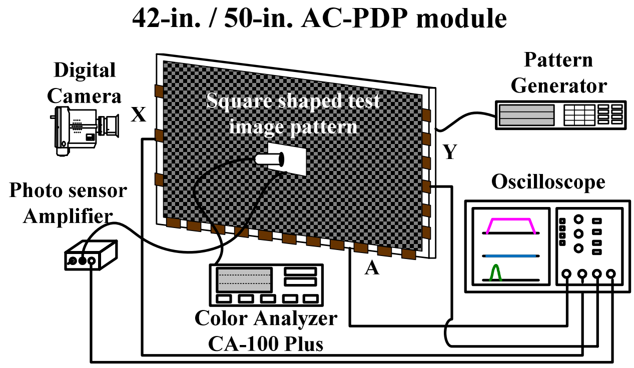

Fig. 1. Schematic diagram of the experimental setup employed in this study.

analyzer (CA-100 plus), and the IR emissions were measured using a photosensor amplifier (C6386). To measure the temporal dark- and bright-image sticking, the entire region of the 50-in panel was changed to black and white backgrounds immediately after a square-type image (discharge region) was displayed at a peak luminance for 30 and 60 s, respectively. Table 1 shows the specifications of the 50-in AC-PDPs that were used in this study: the 50-in HD panel that was used for experiment 1 and the 50-in FHD panel that was used for experiment 2.

Fig. 2 shows the driving waveforms that were applied

Table 1. Specifications of the 50-in HD (Ex. 1)/FHD (Ex. 2) AC-PDP Used in This Study.

<table>
<tr><th colspan="3">Front panel</th><th colspan="2">Rear panel</th></tr>
<tr><td rowspan="2">ITO width</td><td>Ex. 1</td><td>200 μm</td><td rowspan="2">Barrier rib height</td><td rowspan="2">110 μm</td></tr>
<tr><td>Ex. 2</td><td>320 μm</td></tr>
<tr><td>ITO gap</td><td colspan="2">70 μm</td><td>Address width</td><td>90 μm</td></tr>
<tr><td>Bus width</td><td colspan="2">80 μm</td><td>Barrier rib type</td><td>Closed</td></tr>
<tr><td rowspan="2">Pixel pitch</td><td>Ex. 1</td><td colspan="3">576×576 μm</td></tr>
<tr><td>Ex. 2</td><td colspan="3">810×810 μm</td></tr>
<tr><td rowspan="2">Gas chemistry</td><td>Ex. 1</td><td colspan="3">Ne-Xe (11%)-He (0, 35, 50%)</td></tr>
<tr><td>Ex. 2</td><td colspan="3">Ne-Xe (11%)-He (50, 70%)</td></tr>
<tr><td>Pressure</td><td colspan="4">420 Torr</td></tr>
</table>

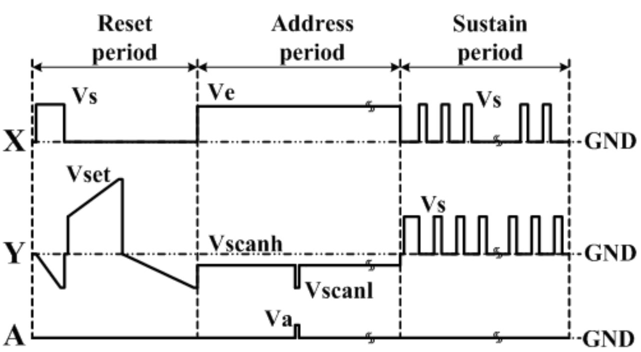

Fig. 2. Schematic diagram of the conventional driving waveform used in this study.

Table 2. Voltage Levels of Each Period Applied at the Three Electrodes.

	[%]	Voltage [V]					
		V_S	V_E	V_A	V_{set}	V_{scanh}	V_{scanl}
Ex.1	He 0	210	110	65	330	-65	-185
	He 35						
	He 50						
Ex.2	He 50	207	110	55	350	-50	-190
	He 70						

to the three electrodes during the reset, address, and sustain periods. The same voltage levels of the driving waveforms were applied to each panel, as shown in Table 2. The frequency for the sustain period was 200 kHz. The ADS driving method was adopted.

3. Experiment Results and Discussion

3.1 Temporal dark-image sticking with various He contents

Fig. 3 and Table 3 shows the square-type test image pattern and measuring point for the investigation of temporal dark-image sticking and the changes in luminance of the discharge and nondischarge regions. To investigate temporal dark-image sticking, a black background was displayed on the screen after a square-type image with peak luminance (914-968 cd/m^2) was displayed for 30 s. Temporal dark-image sticking was observed for several minutes in region B (discharge region). As shown in Fig. 3, the luminance of the discharge region slightly increased with lower He contents, whereas the luminance of the nondischarge region did not change.

To compare the differences in luminance, ΔL was derived based on the luminance before and after discharge ($\Delta L=|L_{before}-L_{after}|$). Fig. 4 shows the differences in luminance and perceived luminance before and after discharge on the dark screen. As shown in Fig. 4, ΔL was slightly

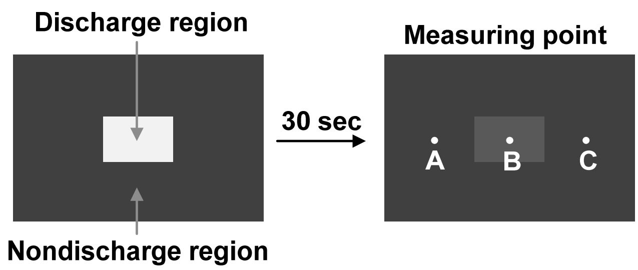

Fig. 3. Square-type test image pattern and measuring point of luminance when displaying a dark screen with various He contents.

Table 3. Changes in Luminance of Fig. 3 Measured before and after the Sustain Discharge when Displaying a Dark Screen with Various He Contents.

	[%]		Luminance [cd/m^2]		
			A	B	C
Ex. 1	He 0	Before	0.24	0.23	0.23
		After	0.24	0.25	0.23
	He 35	Before	0.2	0.19	0.19
		After	0.2	0.2	0.19
	He 50	Before	0.19	0.18	0.17
		After	0.19	0.18	0.17
Ex. 2	He 50	Before	0.4	0.39	0.39
		After	0.4	0.51	0.39
	He 70	Before	0.4	0.4	0.39
		After	0.39	0.42	0.38

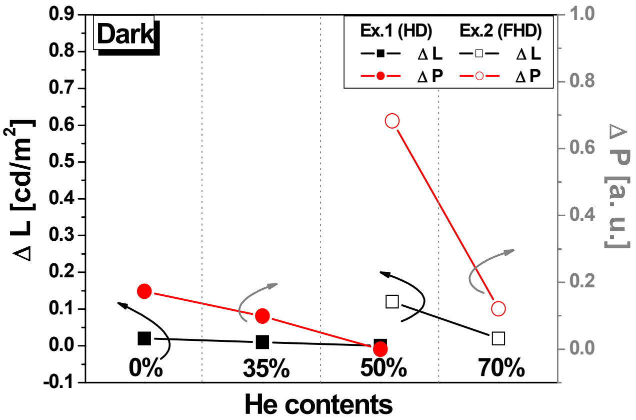

Fig. 4. Differences in luminance and perceived luminance measured before and after discharge in region B (discharge region) on a dark screen with various He contents.

reduced with increased He contents. The maximum differences in luminance were 0.02 and 0.12 cd/m^2 in the 0%- and 50%-He-content HD and FHD panels, respectively. As the human eyes are more sensitive in the dark, the perceived luminance was considered, where the perceived luminance is the luminance perceived by the human eyes. Based on the perceived luminance before and after discharge, ΔP was also derived, where ΔP is the difference in the perceived luminance ($\Delta P=|P_{before}-P_{after}|$). As shown in Fig. 4, the differences in the perceived luminance were significantly reduced with increased He contents.

Fig. 5 shows the changes in IR emissions (828 nm) measured in region B (discharge region) during the reset period. When the IR emissions before discharge were compared with those after discharge, the IR emissions were found to have shifted after discharge. In particular, the shift of the IR emissions was remarkably observed, as shown in Fig. 5(a) for the HD panel and in Fig. 5(d) for the FHD panel. These results indicate that the discharge characteristic was changed by the strong sustain discharge. As shown in Fig. 5, the shift of the IR emissions was significantly observed at lower He contents. To compare the differences in IR emission, the integrated value of the IR emission and the difference in such are shown in Fig. 6. The integrated value of the IR emission was calculated during the same reset period, and the difference in such was derived based on the integrated value of the IR emission before and after discharge ($\Delta I=|I_{before}-I_{after}|$), where I pertains to the integrated value of the IR emission. As shown in Fig. 6, the integrated value of the IR emission increased after discharge in both the HD and FHD test panels. This indicates that the discharge characteristic was changed by the strong sustain discharge. The differences in the integrated value of the IR emission (ΔI) were reduced with increased He contents.

In summary, the differences in luminance and

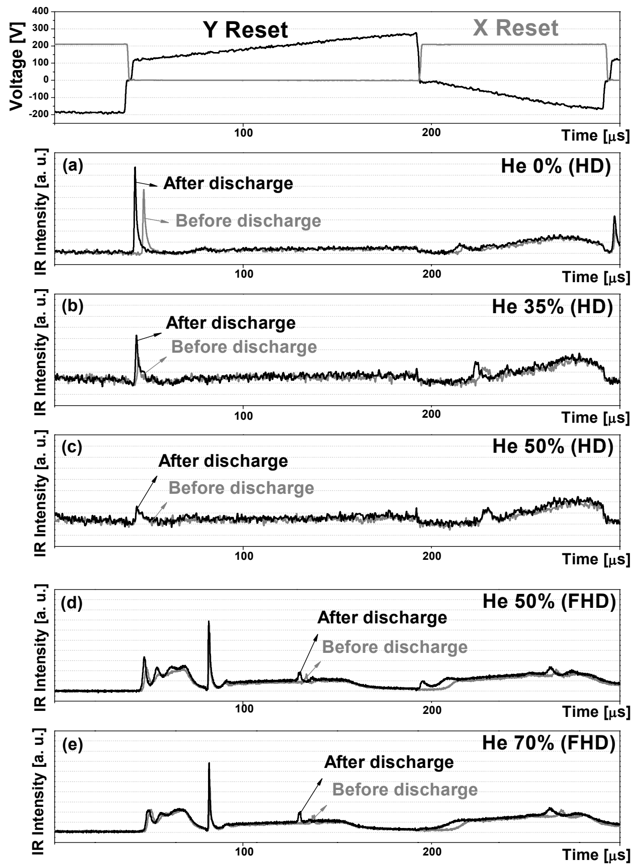

Fig. 5. Changes in IR emission measured from region B during the reset period with various He contents [Ex. 1: (a) 0% He, (b) 35% He, and (c) 50% He; and Ex. 2: (d) 50% He and (e) 70% He].

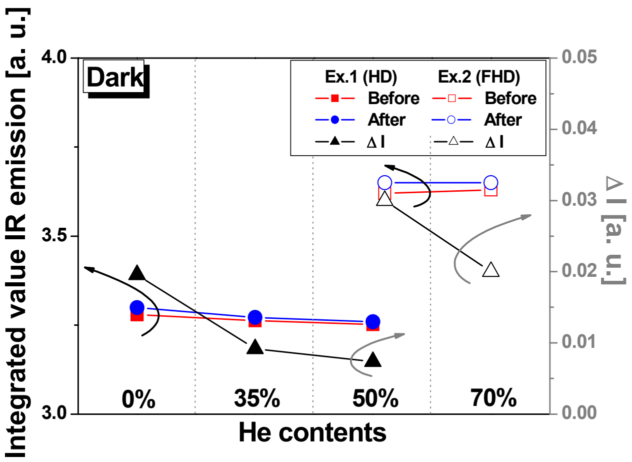

Fig. 6. Differences in the integrated value of the IR emission of region B in Fig. 5 during the reset period with various He contents.

integrated value of the IR emission in the discharge region before and after discharge were observed to have been reduced with higher He contents. In other words, temporal dark-image sticking was reduced with higher He contents. The discharge characteristics for temporal dark-image sticking may thus be deeply related to the reduction of the ions generated during the discharge, which will be further explained later.

3.2 Temporal bright-image sticking with various He contents

Fig. 7 and Table 4 show the square-type test image pattern and measuring point for the investigation of temporal bright-image sticking and the changes in luminance for the discharge and nondischarge regions. To investigate temporal bright-image sticking, a full-white image pattern was displayed on the screen after a square-type image with peak luminance (908-958 cd/m^2) was displayed for 60 s, as shown in Fig. 7(a). Temporal bright-image sticking was observed for several minutes in region B (discharge region), and the luminance of the discharge region was reduced after a square-type image pattern was displayed. These results indicate that the changes in luminance were reduced with higher He contents.

Fig. 8 shows the differences in luminance and perceived luminance before and after discharge on a bright screen with various He contents. To compare the differences in luminance, the luminance of the discharge region before and after discharge are shown in Fig. 8, and the differences in luminance were derived based on these factors

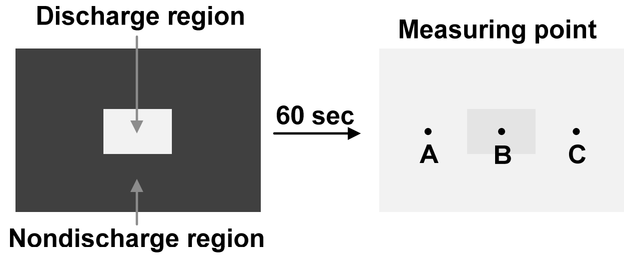

Fig. 7. Square-type test image pattern and measuring point of luminance when displaying a bright screen with various He contents.

Table 4. Changes in Luminance of Fig. 7 Measured before and after the Sustain Discharge when Displaying a Bright Screen with Various He Contents.

	[%]		Luminance [cd/m^2]		
			A	B	C
Ex. 1	He 0	Before	139.2	137.3	135.3
		After	138.4	130.9	134.6
	He 35	Before	139.8	138	139.9
		After	139.5	132.2	139.1
	He 50	Before	144.6	141.5	145.9
		After	144.7	137.4	145.9
Ex. 2	He 50	Before	178.8	178.8	178.7
		After	177.8	172.3	177.9
	He 70	Before	162.8	160.5	161.3
		After	162.6	156.8	161.3

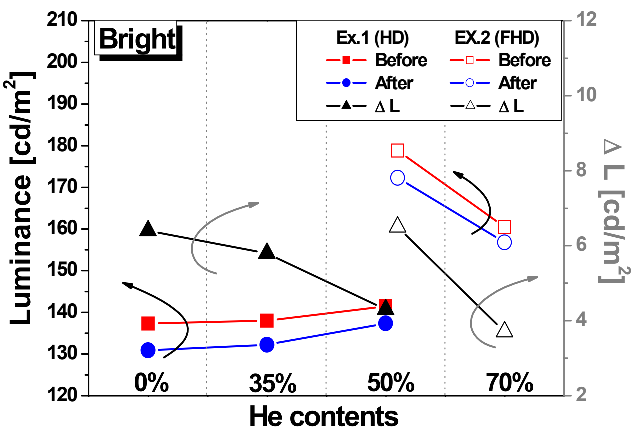

Fig. 8. Luminance and differences in luminance measured before and after discharge in region B on a bright screen with various He contents.

($\Delta L=|L_{before}-L_{after}|$). As shown in Fig. 8, both the luminance and the differences in luminance were reduced in both the HD and FHD test panels. The maximum differences in luminance were 6.4 and 6.5 cd/m^2 for the 0%- and 50%-He-content HD and FHD panels, respectively. Otherwise, the minimum differences in luminance were 4.1 and 3.7 cd/m^2

in the 50%-He-content HD and 70%-He-content FHD panels, respectively. As shown in Fig. 9, the disappearing time was considered for temporal bright-image sticking, where the disappearing time is the time from the start to the completion of the disappearance of temporal bright-image sticking as estimated by the human eyes. The disappearing time in the test panel with low He contents was remarkably long (approximately 80 s) whereas the disappearing time in the test panel with higher He contents was below 30 s.

Fig. 10 shows the changes in IR emissions (828 nm) measured in region B (discharge region) during the sustain period. When the IR emissions before and after discharge were compared, differences in IR emission were observed. In particular, as shown in Fig. 10(a) for the HD panel and in Fig. 10(d) for the FHD panel, the IR emissions showed quite different peaks with higher He contents. This indicates that the discharge characteristic was changed by the strong sustain discharge related to the ion bombardment. To compare the differences in IR emission more precisely, the differences in the integrated value of the IR emission during the sustain period are shown in Fig. 11. The integrated value of the IR emission (I) was calculated during the same sustain period, and the differences in the integrated value of the IR emission were derived based on the integrated value of the IR emission before and after discharge ($\Delta I = |I_{before} - I_{after}|$). As shown in Fig. 11, the integrated value of the IR emission decreased after discharge in both test panels, and the differences in ΔI were reduced with increased He contents.

As the temporal bright-image sticking phenomenon is

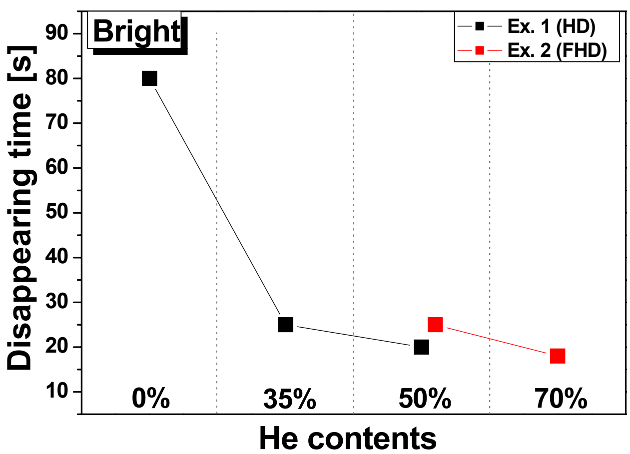

Fig. 9. Disappearing time of the temporal bright-image sticking of the 50-in test panel with various He contents measured by the human eyes.

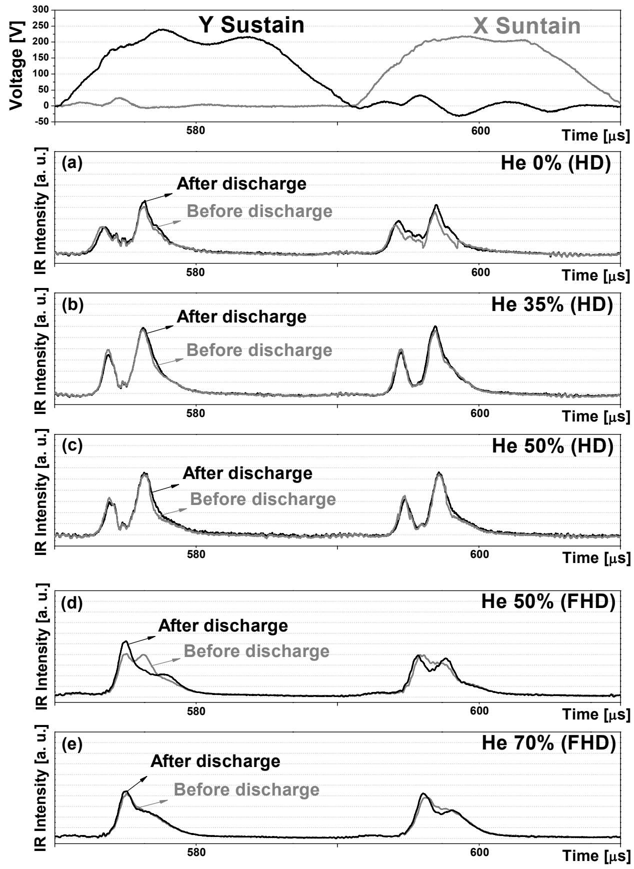

Fig. 10. Changes in IR emission measured from region B during the sustain period with various He contents [Ex. 1: (a) 0% He, (b) 35% He, and (c) 50% He; and Ex. 2: (d) 50% He and (e) 70% He].

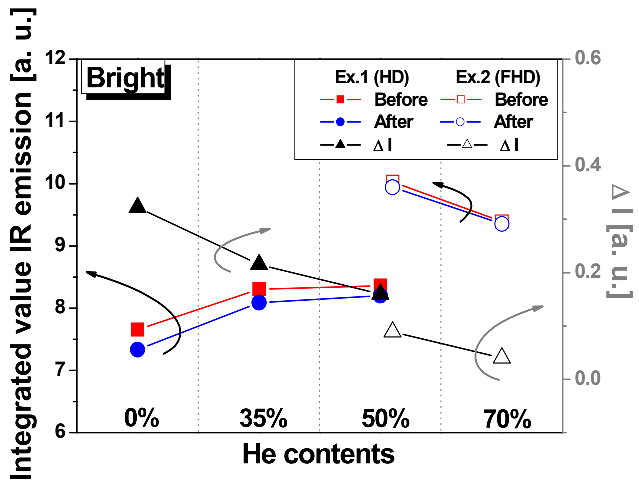

Fig. 11. Differences in the integrated IR emission of region B in Fig. 10 during the sustain period with various He contents.

strongly related to the activation of the phosphor layer, the changes in color coordinate and color temperature in the discharge region before and after discharge are shown in Fig. 12. As shown in Fig. 12(a), the color coordinate tends to shift towards the red or green region after a strong sustain discharge, and the changes in color coordinate were reduced with an increase in He contents. The shift of the color coordinate towards the red region means that the color temperature decreased after a strong sustain discharge, as shown in Fig. 12(b). The differences in color temperature (ΔT) were derived based on the color temperature before and after discharge ($\Delta T = |T_{before} - T_{after}|$). The differences in color temperature before and after discharge were reduced with increased He contents. The differences in luminance, integrated value of the IR emission, color coordinate, and color temperature in the discharge region before and after

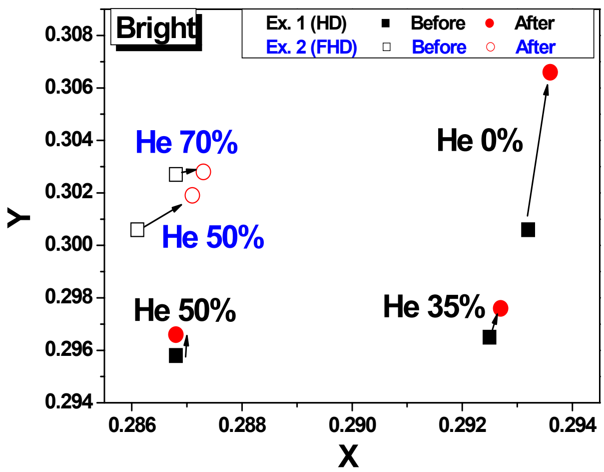

(a)

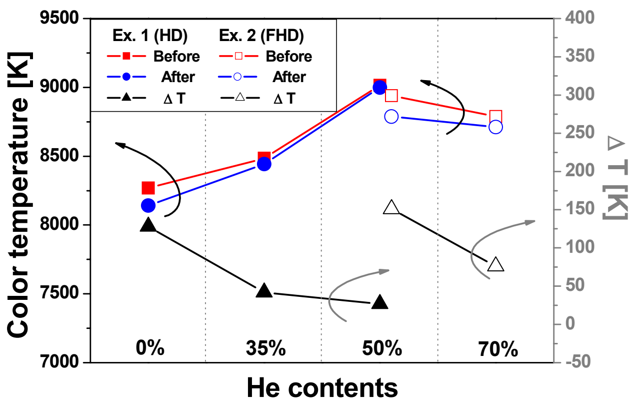

(b)

Fig. 12. Changes in (a) color coordinate and (b) color temperature measured before and after discharge in region B with various He contents.

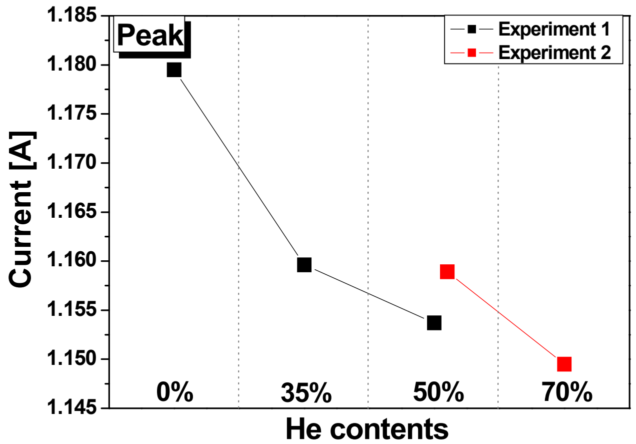

Fig. 13. Changes in the peak current of the 50-in test panel with various He contents used in this study.

discharge tend to be reduced with increased He contents. These results indicate that temporal bright-image sticking was reduced with higher He contents.

Fig. 13 shows the changes in peak current when displaying a square-type image (discharge region) at a peak luminance. As shown in Fig. 13, the peak current was reduced with increased He contents. In the constant Xe % condition, the reduction in the discharge current with an increase in He % means a decrease in the number of ions generated during the discharge [2, 12]. Thus, temporal image sticking may be strongly related to the number of ions generated during the discharge. This experiment result is expected to contribute to the reduction of the temporal dark- and bright-image sticking phenomena in PDP TVs.

4. Conclusions

The temporal dark- and bright-image sticking phenomena were investigated with various He contents in 50-in HD and FHD panels. Based on the experiment data obtained, such as the disappearing time and the differences in luminance, IR emission, color coordinate, and color temperature, the temporal dark- and bright-image sticking was observed to have been reduced with an increased He % in the ternary-gas-mixture condition. It is expected that the proposed high He gas condition can achieve high image quality, thanks to the reduction of the temporal dark- and bright-image sticking in the ac-PDPs.

References

[1] S.-K. Kwon, J.-H. Kim, S.-K. Moon, J.-K. Choi, Y.-I. Jang, K.-H. Park, & S.-S. Han, *In Proc. SID'09 Dig.* (2009), p.359.

[2] K.-H. Park, H.-S. Tae, H. S. Jeong, M. Hur, & E. G. Heo, *J. of Soc. Information Display* **17**, 61 (2009).

[3] H.-S. Tae, C.-S. Park, B.-G. Cho, J.-W. Han, B. J. Shin, S.-I. Chein, & D. H. Lee, *IEEE Trans. Plasma Sci.* **34**, 996 (2006).

[4] J. H. Kim, C.-S. Park, B.-S. Kim, K.-H. Park, & H.-S. Tae, *Journal of Information Display* **8**, 29 (2007).

[5] C.-S. Park, B.-G. Cho, & H.-S. Tae, *Journal of Information Display* **9**, 39 (2008).

[6] C.-S. Park & H.-S. Tae, *IEICE Trans. Elec.* **E-92C**, 161 (2009).

[7] B. J. Shin, K. C. Choi, & J. H. Seo, *IEEE Trans. on Elec. Dev.* **52**, 17 (2005).

[8] S. H. Kim, K. C. Choi, & B. J. Shin, *In Proc. IDW'05 Dig.* (2005), p.1555.

[9] H.-J. Lee, D.-H. Kim, Y.-R. Kim, M.-S. Hahm, D.-K. Lee, J.-Y. Choi, C.-H. Park, J.-W. Rhyu, J.-K. Kim, & S.-G. Lee, *In Proc. SID'04 Dig.* (2004), p.214.

[10] J. H. Choi, Y. Jung, K. B. Jung, S. B. Kim, P. Y. Oh, H. S. Jung, K. Y. Sung, & E. H. Choi, *In Proc. IDW'03 Dig.* (2003), p.913.

[11] M. J. Jeon, M. S. Chung, S. C. Lee, K. S. Lee, J. S. Kim, & B. K. Kang, *Displays* **30**, 39 (2009).

[12] K.-H. Park, H.-S. Tae, H. S. Jeong, M. Hur, & E. G. Heo, *IEEE Trans. on Plas. Sci.* 17, 61 (2009).